CMA/NSMC Satellite Data Assimilation Activities: Uses of ATOVS and Fengyun VASS Data in WRF

Lu Qifeng[1], Liu Zhiquan[1,2],Wu Xuebao[1], Zhang Peng[1], Lu Naimeng[1], Zhang Fengying[1], Ma gang[1,] Yang jun[1], Dong Chaohua[1], Tang shihao[1], Dale Barker[2]

[1]National Satellite Meteorological Center, CMA
[2]NCAR/MMM
E-mail: luqf@cma.gov.cn, lqifeng@163.com

ABSTRACT

The regional ATOVS data received and preprocessed by National Satellite Meteorological Center of Chinese Meteorological Administration (NSMC/CMA) have been operationally assimilated in NSMC/CMA using regional 3DVar data assimilation system (WRF/3DVar) by RTTOV8.7 model. Based on the WRF 3DVAR system of NCAR, some improvements were further done to put the satellite data into use in NWP model at NSMC/CMA. In this paper, the extensions on WRF 3DVAR for satellite data assimilation at NSMC/CMA were introduced; the assimilation application of ATOVS data in the typhoon track prediction and in emergency response to monitor the snow storm occurred in January 2008 over South China were demonstrated; further the potential of FY3 VASS data assimilated into NWP was analyzed; and finally the further work on the satellite data assimilation was delineated.

Key words: **CMA/NSMC, Satellite Data Assimilation Activities, ATOVS, FENGYUN VASS**

1 INTRODUCTION

The regional ATOVS data was received and preprocessed by National Satellite Meteorological Center of Chinese Meteorological Administration (NSMC/CMA) and the ATOVS radiances have been operationally assimilated (Liu, 2006) in NSMC/CMA using regional 3DVAR data assimilation system (WRF/3DVar, Barker, 2004, 2006) by RTTOV8.7 model (Eyre, 1991). WRF 3DVAR system was developed from MM5 3DVAR system, the more details on the WRF and WRF 3DVAR can be found in reference of WRF model guidance (Michalakes et. al., 1999; William et. al., 2006).

Based on the WRF 3DVAR system of NCAR, the following works were further done to improve the satellite data application in NWP model at NSMC/CMA.

1). The satellite atmosphere data assimilate system was constructed based on WRFV2 forecast model and 3Dvar assimilation system, with the assimilation system forced by NCEP and T213 dataset, with 6-hour assimilation window at 00, 06, 12, 18UTC, corresponding to 21-03, 03-09, 09-15, 15-21UTC, and post-processed by NCAR-GRADS, and extends them as following：
   - With RTTOV8.7 for radiance assimilation；
   - Using Harris & Kelley Method (Eyre, 1992; Harris and Kelly, 2001) for bias correction；
   - Using NMC Method for background covariance；
   - Modifying land surface dataset for China surface complexity；
   - Using ATOVS data received, preprocessed by NSMC/CMA;
   - With More reasonable algorithm to retrieve typhoon track
   - With BE updated every 6 hour;
   - With corresponding physics schemes selected to depict the snow information

- With FY3/VASS instruments added into WRF/3Dvar;
- With METOP/IASI instrument added into WRF/3Dvar.

2). Tentatively build the operational procedure of assimilation and prediction for typhoon utilizing the assimilation system already set up, with some valuable results obtained.

3). Develop the preliminary emergency service procedure to monitor snow storm based on ATOVS assimilation, which has been applied to monitor the snow storm occurred in South China in JAN 2008.

4). Tentatively set up the satellite assimilate procedure for FY3/VASS data.

WRF model is executed daily at NSMC/CMA, providing forecasts over China, with initial data taken from T213 global model, kindly provided by the National Meteorological Center of Chinese Meteorological Administration (NMC/CMA). WRF updates 4 times per day and produce forecast for 48 hours to the future. Forecasts include wind speed and direction, wind gusts, temperature, total cloud cover and precipitation etc.

In this study, the data assimilation experiments were conducted before and after the operational use of ATOVS radiances to demonstrate significant impacts on forecasts and analyses of typhoon track and the application case of assimilating ATOVS to monitor the snow storm occurred in January 2008 were demonstrated, finally the application potential of FY3 VASS in typhoon track prediction was analyzed.

2 ATOVS ASSIMILATION AND ITS APPLICATION IN TYPHOON TRACK PREDICTION

2.1 Bias correction

The statistical feature of scan angle bias in all channels of ATOVS/NOHAA18 HIRS4, AMSU-A and MHS has been statistically analyzed, as showing in Fig 2 with the scan angle bias of channel 1-15 of ASMU-A varying along scan position, revealing that the scan angle bias generally increase with the scan position far away from the nadir, but not increase strict-progressively; the scan angle bias of some channel take on opposite change tendency of scan angle bias at the both sides of nadir. All this further verify the importance of scan angle bias correction.

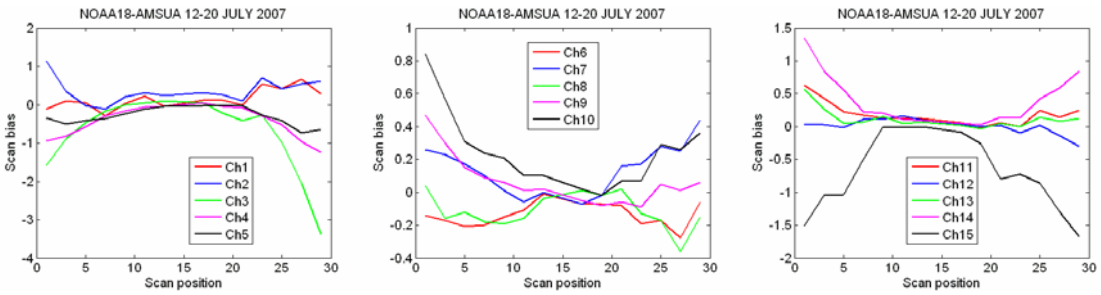

Fig 1 the scan angle bias of AMSU-A

The correction coefficients calculated from statistical samples of some time before always are utilized to correct the brightness temperature biases at the nest time, further used into the radiance assimilation system. In this study the correction coefficients were calculated from statistical samples from 10 July to 10 August 2007 to correct brightness temperature bias after 10 August, with the brightness temperature bias before correction and after at 0600UTC 15 August plotted in Fig4, indicating that the results of bias correction is encouraging, the statistical distribution of brightness temperature bias after correction locates mostly in the vicinity of zero, with the more Gaussian distribution, especially obvious for the some “bad ” channel, such as 1-3, and 13-15. The bias correction was not always perfect, such as, for channel 11 and 12 with asymmetric distribution, and for

channel 13 and 14 with bimodal distribution structure, which maybe resulted from the error of channel itself, and could not be dispelled through bias correction itself.

The results of brightness temperature bias correction of HIRS and MHS were similar to AMSU-A, no more details were given here due to the limited space.

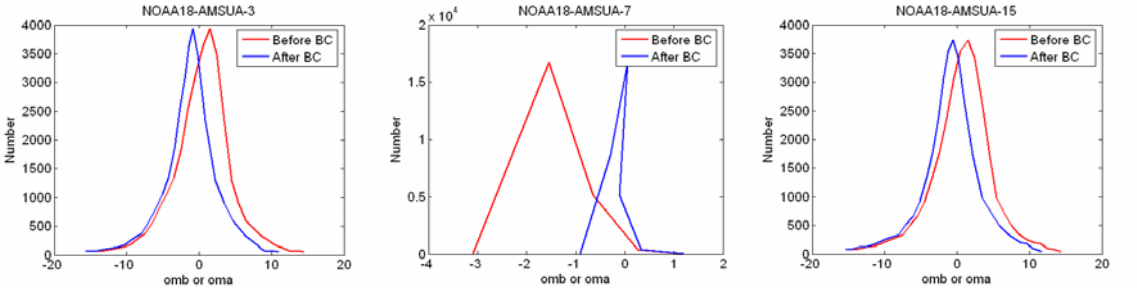

Fig 2 brightness temperature bias distribution before and after correction

2.2 Assimilating ATOVS data

It could be seen from Fig 3 that the predicted typhoon track without the ATOVS assimilation leans more northwards than the observed one, while the predicted typhoon track with the ATOVS assimilation was adjusted southwards, with better agreement with the observed one, but during the period at the initial stage and after the landfall of typhoon, the typhoon track with ATOVS assimilation and without all could not be simulated well. The reasons may be that, at initial stage, because there exist large area of positive scattered vorticity, the typhoon track retrieval algorithm used here can not find and discriminate the correct track from so many positive vorticity; after landfall, due to the complexity of land surface characteristic, which will inspire some meso- or small-scale convection weather system, and because the landfall system would be reduced fast, it is difficult to distinguish the landfall system from the inspired system using the minimum vorticity method, leading to less accuracy for the typhoon track retrieval.

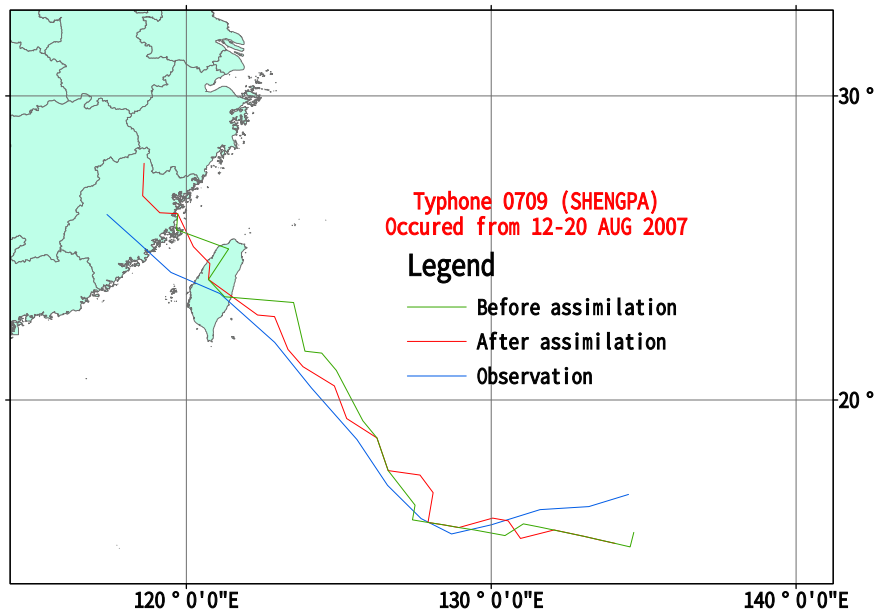

Fig 3 the predicted typhoon track with and without the ATOVS assimilation

3 ATOVS ASSIMILATION TO MONITOR 2008 SNOW STORM IN SOUTH CHINA

In the middle and last ten days of January 2008, the southern area of China was attacked by the snow storm,

leading to paralysis of traffic and communication, which make the rescue work more difficult.

At the critical time to rescue, observation information from the surface radar and surface station could not be provided for sufficient data or was delayed due to the snow storm, though the snow cover information can be obtained from satellite observation in visible and infrared spectral channel, quantitative snow information to monitor snow storm still rely on the observation from the microwave sensor, such as SSM/I or SMMR, however, during the snow storm in January 2008, this observation could be obtained in real-time, leading to no real-time effect snow information provided from this datasets. The ATOVS data was received and preprocessed by NSMC/CMA in real-time, with no more than half an hour from receiving to preprocessing, which make it possible to provide the snow disaster information controlled by the weather background at regional scale.

In this study the ATOVS data was assimilated to provide more accurate snow information, by carefully selecting physical schemes, with the NOAH land surface sub-model selected to delineate the physics mechanism of snow-frozen and snow-melting.

In the figure of geo-potential height and temperature at 500hPa on 0600UTC 28 January 2008, there clearly existed one steady block high pressure in the vicinity of Ural mountain, and one horizontal trough at southern side of Baikal, with -42^{o}C as its corresponding temperature, and the dry and cold air current after trough flows southwards along the small fluctuation of middle latitudes at south side of block high pressure, with straight circulation of middle latitudes and prevailing westward wind; at the same time, there exist one trough eastward near 96^{o}E, with the temperature trough lagging behind the atmospheric pressure trough, and there is obvious cold laminar flow after the trough; The powerful northwest pacific subtropical high over southeast of China makes the southward current of blocky high, trough current and subtropical high form tripartite equilibrium situation over south area of China, with heavy snowfall weather course over the interface region of the three.

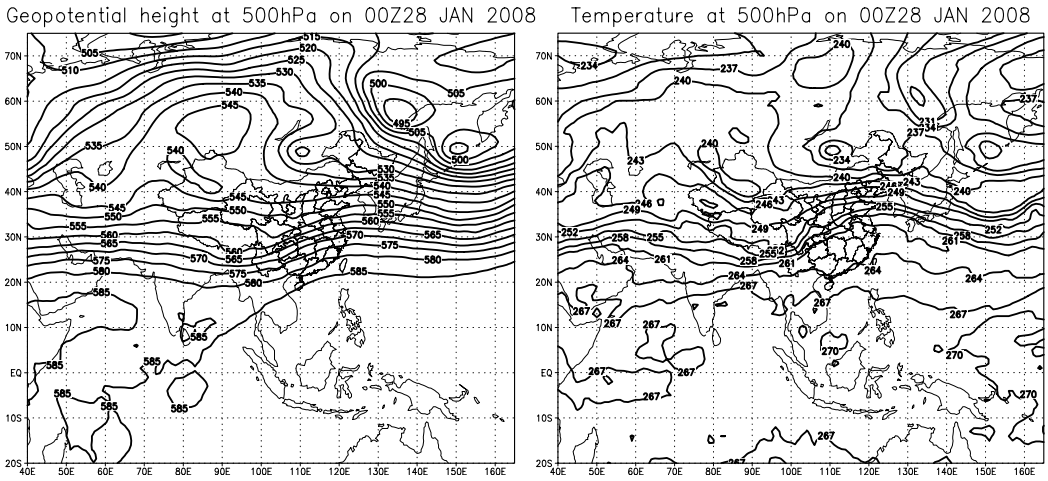

a. Geo-potential height at 500hPa ; b. Temperature contour at 500hPa

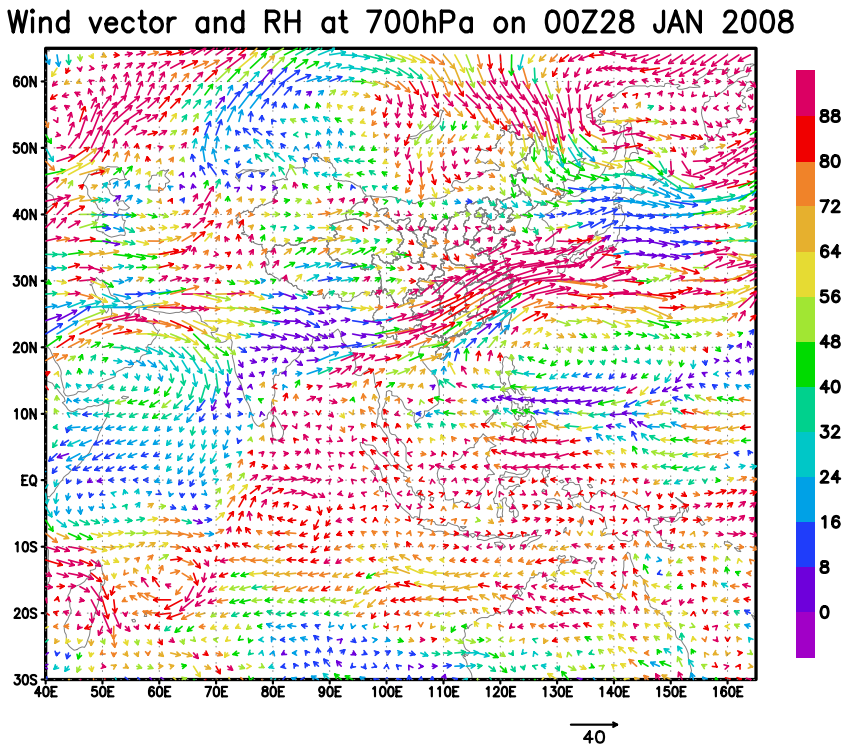

c. Wind and water vapor at 700hPa

Fig.4 Synoptic background on 28 JAN 2008

It could be seen from the figure of wind field and water vapor field at 700hPa that the strong air current from Europe-Atlantic Ocean was divided into two pieces of north and south, with north piece northward into the polar region of high latitude, invading China with colder momentum, leading to the stronger northwest monsoon, and with south piece southward into Central Asia forming the low vortex, with the air current at the side of low vortex moving round Qinghai-Tibet Plateau into Bay of Bengal and further into China border, leading to the more violent warm-wet current invaded from south and with a water vapor transportation zone along Northeast-Southwest direction formed over the South China.

Fig 5 demonstrate the corresponding relations between the observed snow depth over snow storm area of South China and the observed brightness temperature at channel 5 of ATOVS/NOAA18-MHS on 0600UTC 28 January 2008, with the brightness temperature at channel 5 reflecting the characteristics of water vapor transportation and functionally weighted at 700hPa as background, and in the figure, the green triangle stands for the station with snow depth more than 12cm observed on 0600UTC 28 January 2008, while the red dot for the station with snow depth less than 12cm.

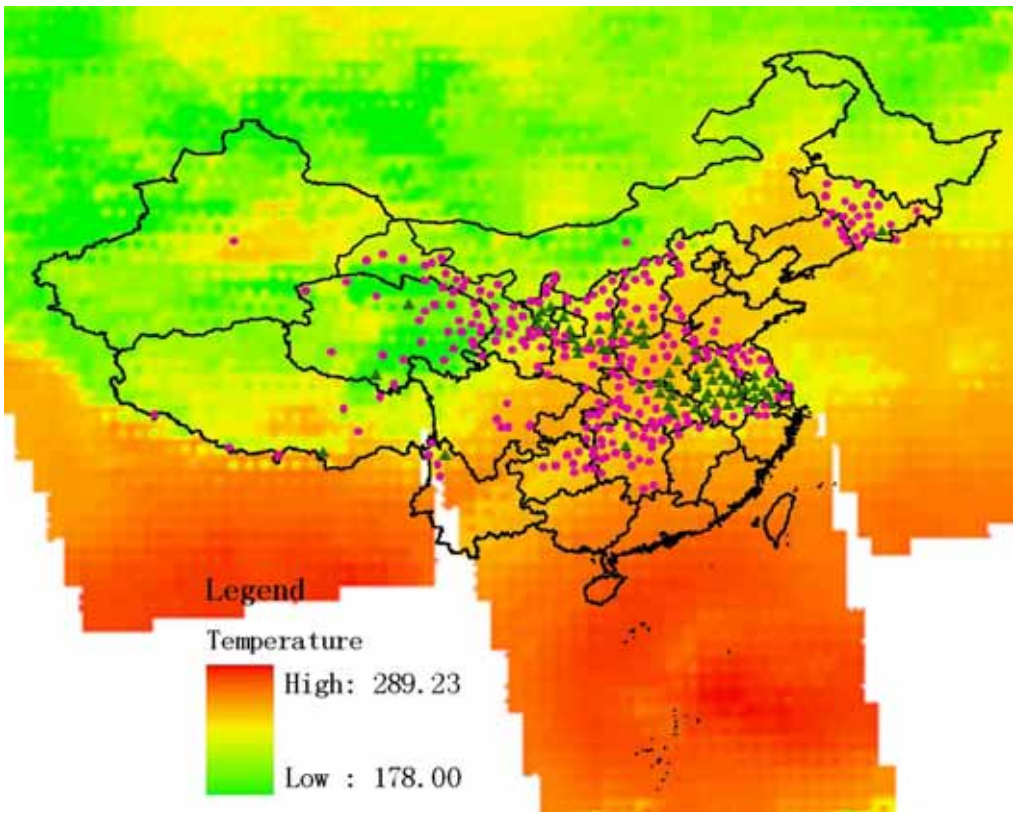

Fig. 5 Composition chart of observed snow depth and Bright Temperature at channel 5 of ATOVS/NOAA18-MHS

It can be seen from the Fig 5 that there exist cold zone in Southwest-Northeast direction from along Yunnan-Guizhou to Changjiang-Huaihe, which corresponds to the water vapor transportation zone at 700hPa from Indian ocean to Bay of Bengal into South China; The cold area in the background of observed brightness temperature correlates well to the area of heavy snowfall observation, with lower brightness temperature over the area of Changjiang-Huaihe corresponding to the more heavy snowfall; at the same time, the brightness temperature decreases over large area from Gansu-Shanxi to North China caused by the invasion of colder air current from Siberia into China, with the heavy snowfall over large area actually observed.

The comparison analysis between brightness temperature in channel 5 of ATOVS/NOAA18-MHS and snow depth observation demonstrate that: the information on temperature decrease and snowfall was contained in the satellite-observed ATOVS data, with one confirming another well. The forecast system simulates and predicts the spatial-temporal development of weather situation based on dynamics mechanism, and theoretically the more accurate snowfall information such as snow depth and snow water equivalence could be simulated by assimilating the ATOVS data containing the snowfall information and under full consideration of the physical process of snow-freezing and snow melting.

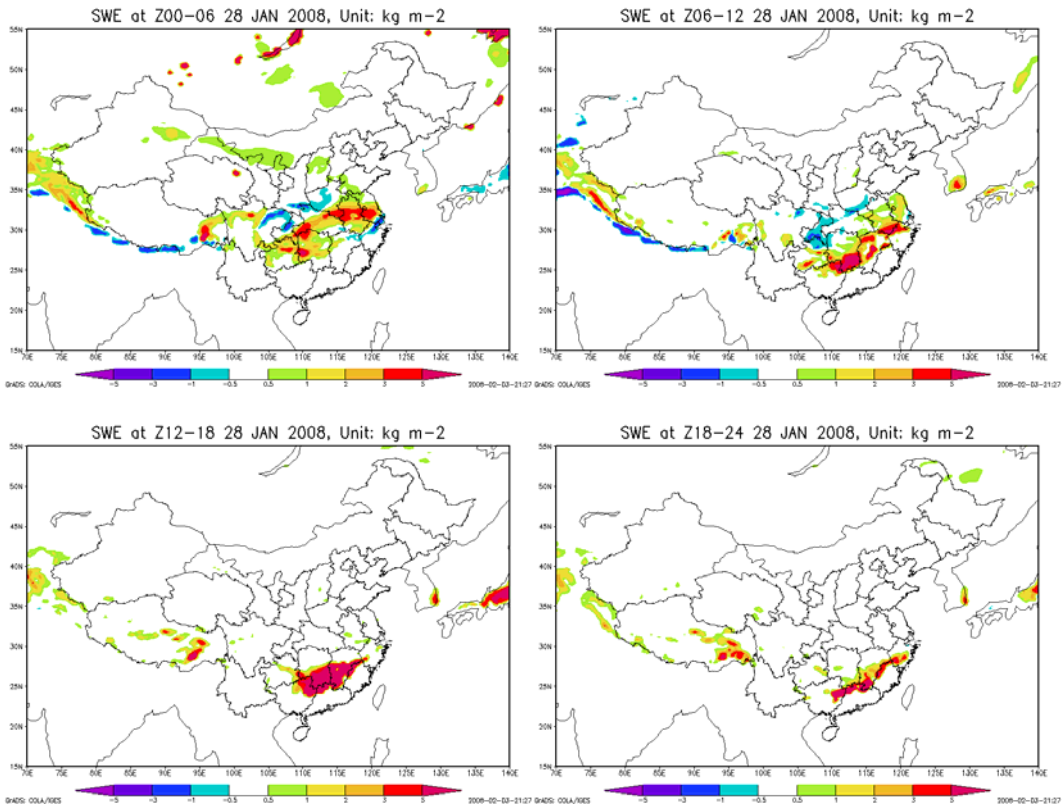

Fig.6 6hr evolvement chart of snow water equivalence during 0000UTC to 0024 UTC 28 JAN 2008

The variable in Fig 6 stands for the snow water equivalent change in 6 hours at 00-06, 06-12, 12-18, and 18-24UTC (Unit: kg/m^2), with positive value for snow-precipitating in 6 hours and with negative value for snow-melting in 6 hours. As the lower trough at 500hPa move eastwards and colder air current after the trough move southwards, the strong shear line has been formed, moving east-southwards, leading to the snowfall area to move east-southwards gradually too. The results from Fig 4 delineate this evolution tendency, which demonstrates that this snowfall event was caused by the weather process and the change tendency of snow water equivalent in 6 hours could reflect the moving track of weather process.

4 FY3-VASS DATA ASSIMILATION AND ITS RELATED

The FY3 will be launched soon (at the end of May 2008), with vertical atmospheric sounder system (VASS) on-boarded, including InfRared Atmospheric Sounder (IRAS), Microwave humidity sounder (MWHS), and Microwave temperature sounder (MWTS). These instruments are similar to ATOVS instrument of NOAA series and the instrument IRAS, MWTS and MWHS of FY3 VASS, theirs Passband Characteristic and theirs counterparts in NOAA ATOVS are shown in Table 1, 2, 3. Before FY3 launched, we adopt the similar channels of NOAA ATOVS to carry on research.

Table 1 FY3 IRAS Channels, Its Passband Characteristic and Its counterparts in NOAA18

FY3-IRAS		NOAA-18-HIRS					
chan	Center number (cm^{-1})	chan	Center number (cm^{-1})	center wavelengh (μm)	Half-width (cm^{-1})	absorbers	Largest contribution (hPa)
1	669	1	669	14.95	3	CO_2	30

2	680	2	680	14.71	10	CO_2	60
3	690	3	690	14.49	12	CO_2	100
4	703	4	703	14.22	16	CO_2	400
5	716	5	716	13.97	16	CO_2	600
6	733	6	733	13.64	16	CO_2/H_2O	800
7	749	7	749	13.35	16	CO_2/H_2O	900
8	802	10	802	12.47	30	window	surface
9	900	8	900	11.11	35	window	surface
10	1030	9	1030	9.71	25	O_3	25
11	1345			7.43	50	H_2O	800
12	1365	11	1365	7.33	40	H_2O	700
13	1533	12	1533	6.52	55	H_2O	500
14	2188	13	2188	4.57	23	N_2O	1000
15	2210	14	2210	4.52	23	N_2O	950
16	2235	15	2235	4.47	23	CO_2/N_2O	700
17	2245	16	2245	4.45	23	CO_2/N_2O	400
18	2388	17	2420	4.19	25	CO_2	atmosphere
19	2515	18	2515	3.98	35	window	surface
20	2660	19	2660	3.76	100	window	surface

Table 2 FY3 MWTS Channels, Its Passband Characteristic and Its counterparts in NOAA18

FY3-MWTS		NOAA-18-AMSUA				
Chan num	Center frequen (GHz)	Chan Num	Center frequen (GHz)	Width (MHz)*	absorber	Largest contribut
1	50.30	3	50.30	161.14	window	surface
2	53.596±0.115	5	53.596±0.115	168.20	O_2	600 hPa
3	54.94	7	54.94	380.56	O_2	250 hPa
4	57.290	9	f_0=57.30	310.42	O_2	80 hPa

Table 3 FY3 MWHS Channels, Its Passband Characteristic and Its counterparts in NOAA16

FY3-MWHS		NOAA-16-AMSUB				
Chan num	Center fre (GHz)	Chan Num	Center fre (GHz)	halfwid (MHz)	absorb	Largest contribu
1	150(V)	1		1000	window	surface

2	150(H)	2	150.00(H)	1000	window	surface
3	183.31±1	3	183.31 ±1	500	H20	350 hPa
4	183.31±3	4	183.31 ±3	1000	H20	500 hPa
5	183.31±7	5	183.31 ±7	2000	H20	650 hPa

Fig 4 showed that by adopting the bias correction of Harris and Kelly, the statistical distribution of brightness temperature bias after correction locates mostly in the vicinity of zero, with the more Gaussian distribution.

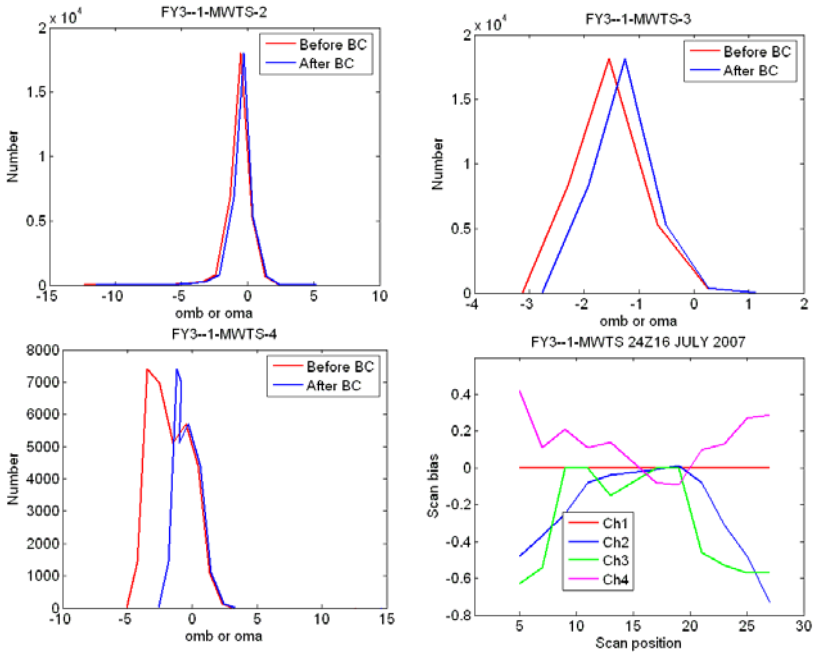

Fig 7 brightness temperature bias distribution before and after correction for FY3 VASS MWTS

The observed geo-potential height at 500hPa and the difference of geo-potential height at 500hPa after and before assimilating FY3 VASS at 500hPa were demonstrated in Fig 8 and Fig 9 respectively. In Fig 9, the green contour line was utilized to indicate the simulated geo-potential height at 500hPa without assimilating FY3 VASS data, to clearly display the effect of assimilating the FY3 VASS data, the difference between geo-potential height at 500hPa after and before assimilating FY3 VASS was drawn, with the blue dotted line standing for negative difference between the two, and with the filled area for positive difference between the two.

Comparison of the simulated geo-potential height at 500hPa without assimilating FY3 VASS data in Fig 9 with observed one in Fig 8 demonstrate that the trough in the Northwestern China was overestimated, with shallower trough predicted and the ridge in the Southeast China was underestimated, with weaker ridge predicted. It can be seen from the difference between geo-potential height at 500hPa after and before assimilating FY3 VASS in Fig 9 that after assimilating FY3 VASS, the deeper trough and the stronger ridge was simulated than before assimilating FY3 VASS, in better agreement with the observed one.

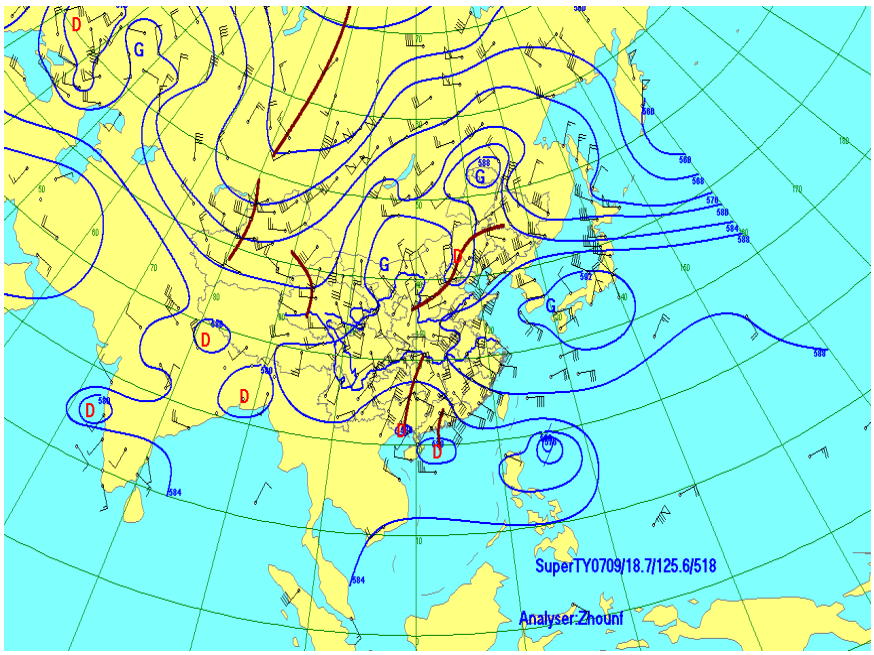

Fig 8 observed geo-potential height at 500hPa

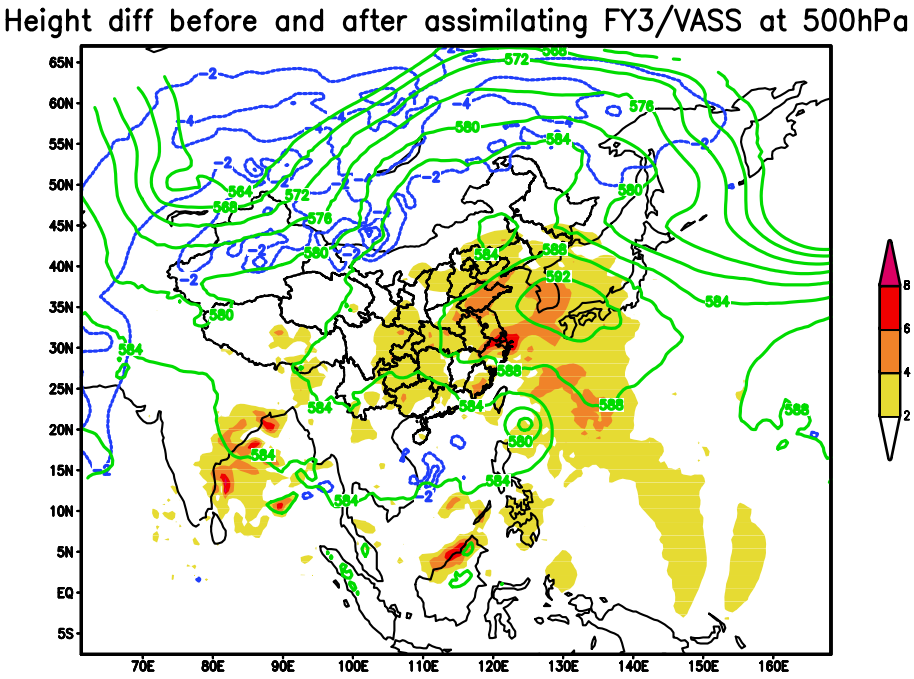

Fig 9 difference of geo-potential height at 500hPa after and before assimilating FY3 VASS at 500hPa

5 CONCLUSION AND FUTURE WORK

In this study, the extensions to the WRF 3DVAR system done at NSMC/CMA for the better using satellite data into NWP was overviewed, the ATOVS assimilation application in typhoon track prediction and in emergency response to monitor the snow storm occurred in January 2008 over South China were demonstrated, indicating that by assimilating ATOVS data, the prediction skill can be improved well and more accurate information can be provided to monitor disaster. The preliminary results of FY3 VASS data assimilation based on NOAA ATOVS suggest that the simulation could be improved by

assimilating the FY3 VASS data and the potential of FY3 VASS application in NWP model is great.

Although the frame of satellite data assimilation has been established and the preliminary results are inspiring, there are still many detail questions needed to solve, such as the inaccuracy of emissivity leads to discard so many radiance, especially in Tibet Plateau region and cloudy contamination reduce the effect information into the assimilation system. To solve these questions, the future work will focus on the following:

- **The core work on satellite data assimilation of** NSMC/CMA orientate on quality control and bias correction.
- **Directly assimilate the radiance** by RTTOV and CRTM fast radiative transfer model; Assimilate the atmospheric profile of temperature and moisture from FY3A, cloud track wind, and ocean surface wind by the interpolation algorithms; provide the input for fast radiative transfer model by setting up the dynamic O3 datasets.
- **The inaccuracy of land surface emissivity** leads to less radiance data assimilated into in Plateau region of China and discarding the radiance in the window channel, to solve this, the following scheme was adopted: For the infrared spectral region, the land surface emissivity needed by HIRS data assimilation was convolved from the one of high spectrum; For the microwave spectral region, the 1DVAR method can be used to obtain land surface emissivity.
- **Assimilating the radiance in the cloudy region:** ***a.*** The radiance always was discarded in infrared spectral region due to the cloudy contamination during radiance assimilation, however, the radiance in the cloudy region contain some atmospheric information on the cloud, so it is valuable to assimilate the infrared radiance in the cloudy region, implementing as following: First of all, compare the cloud physical schemes to select the prefect one, by which (provide the cloud parameters needed by RTTOV) the RTTOV will simulate the radiance, with smallest error comparing between observed radiance and simulated one; Utilize LAPS cloud analysis scheme to obtain more accurate cloud top emissivity and cloud parameters need by RTTOV to simulate cloudy radiance, and then assimilate the cloudy radiance by fast radiative transfer model. ***b.*** For precipitating cloud radiance, assimilate the cloudy radiance derived by scatter module in fast radiative transfer model using the cloud top emissivity and cloud parameters above.

ACKNOWLEDGMENTS

This work was supported by Natural Science Foundation of China (Grant No. 40705037), PLA General Armament Department Pre-research Project (Grant No. 0605513220503), National High Science & Technology Development Plan of China (863 Plan, Project: 2006AA12Z148), and The Open fund by Numerical Model Innovation base of China Meteorological Administration (Agreement 2006-12), “Applying High resolution land surface data into meso-scale numerical model”.

REFERENCE

Barker, D. M., W. Huang, Y.-R. Guo, A. Bourgeois, and X. N. Xiao, 2004: A Three-Dimensional Variational Data Assimilation System for MM5: Implementation and Initial Results Mon. Wea. Rev., 132, 897–914.

Barker, D. M., Bray, J., Guo, Y., et al. Status report on WRF-ARW's Variational Data Assimilation System (WRF-VAR)[J]. 7th WRF Users' Workshop, 2006.

Eyre, J. R.. A fast radiative transfer model for satellite sounding systems. In ECMWF Tech Memo, 1991, pp. 176.
Eyre, J. R. A bias correction scheme for simulated TOVS brightness temperatures. In Technical Memorandum, ECMWF, 1992, pp. 28.
Harris, B. A., Kelly, G. A satellite radiance bias correction scheme for radiance assimilation[J]. Q J R Meteorol Soc, 2001, 127:1453-1468.
Liu, Z., Barker, D. M. Radiance assimilation in WRF-Var: Implementation and initial results[J]. 7th WRF Users' Workshop, 2006.
Michalakes, J., Dudhia, J., Gill, D. Design of a next-generation regional weather research and forecast model[J]. Towards Teracomputing, World Scientific, River Edge, New Jersey, J Klemp, and W Skamarock, 1999:117-124.
William, C. S., Joseph, B. K., Jimy, D., et al (2008). A Description of the Advanced Research WRF Version 3 (Boulder, NCAR TECHNICAL NOTE NCAR), pp. 126